

Synthesis and Preliminary Evaluation of ^{18}F - or ^{11}C -Labeled Bicyclic Nucleoside Analogues as Potential Probes for Imaging Varicella-Zoster Virus Thymidine Kinase Gene Expression Using Positron Emission Tomography

Satish K. Chitneni,[†] Christophe M. Deroose,[‡] Jan Balzarini,[§] Rik Gijsbers,^{||} Sofie J. L. Celen,[†] Tjibbe J. de Groot,[‡] Zeger Debyser,^{||} Luc Mortelmans,[‡] Alfons M. Verbruggen,[†] and Guy M. Bormans^{†,*}

Laboratory for Radiopharmacy, Faculty of Pharmaceutical Sciences, K.U. Leuven, Leuven, Belgium, Department of Nuclear Medicine, K.U. Leuven, Leuven, Belgium, Rega Institute for Medical Research, K.U. Leuven, Leuven, Belgium, and Division of Molecular Medicine, K.U. Leuven, Leuven, Belgium

Received August 9, 2006

Two radiolabeled bicyclic nucleoside analogues (BCNAs) were synthesized, namely 3-(2'-deoxy- β -D-ribofuranosyl)-6-(3-[^{18}F]fluoroethoxyphenyl)-2,3-dihydrofuro[2,3-*d*]pyrimidin-2-one (^{18}F -**2**) and 3-(2'-deoxy- β -D-ribofuranosyl)-6-(3-[^{11}C]methoxyphenyl)-2,3-dihydrofuro[2,3-*d*]pyrimidin-2-one (^{11}C -**3**), and evaluated as PET reporter probes for varicella-zoster virus thymidine kinase (VZV-tk) gene expression imaging in brain. ^{18}F -**2** and ^{11}C -**3** were synthesized starting from phenol precursor **1**. The phenol precursor **1** was converted to stable as well as to radiolabeled compounds **2** and **3** using $^{19/18}\text{FCH}_2\text{CH}_2\text{Br}$ or $^{12/11}\text{CH}_3\text{I}$ as alkylating agent. In vitro evaluation of ^{18}F -**2** and ^{11}C -**3** in 293T cells showed a 4.5 and 53-fold higher uptake, respectively, into VZV-tk gene-transduced cells compared to control cells. However, biodistribution studies in mice demonstrated low uptake of these tracers in the brain. RP-HPLC analysis of plasma and urine samples of mice injected with ^{11}C -**3** revealed that this tracer is very stable in vivo. These data warrant further evaluation of these tracers as noninvasive imaging agents for VZV infection and VZV-tk reporter gene expression in vivo.

Introduction

Molecular imaging is a rapidly developing field at the convergence of several disciplines. The basic goal of any molecular imaging study is to monitor the expression, activity, or function of a specific molecular target, using a suitable probe to visualize and characterize the target by means of a suitable imaging system such as positron emission tomography (PET^a). A paradigm for noninvasive reporter gene imaging using radiolabeled probes was initially described by Tjuvajev et al. in 1995. This paradigm requires an appropriate combination of a reporter transgene and a reporter probe, where the reporter gene product (an enzyme) selectively converts the reporter probe to a metabolite that is trapped within the transduced cell.^{1,2} When the reporter gene is linked to another (e.g., therapeutic)

transgene, the accumulation of reporter probe in tissues can be used to measure the magnitude, location, and timing of expression of the transgene.³ In vivo model systems have been developed and validated using the wild type herpes simplex virus type 1 thymidine kinase (HSV1-tk) gene and a mutant HSV1-tk gene, HSV1-sr39tk, as PET reporter genes, in combination with several radiolabeled acyclo-guanosine and pyrimidine nucleoside analogues as PET reporter probes. Most of the radiolabeled pyrimidine nucleoside PET reporter probes have used iodine-124 as a radiolabel (e.g., 2'-deoxy-2'-fluoro-5-iodo-1- β -D-arabinofuranosyluracil (FIAU)). The long half-life of iodine-124 (4.18 days) allows longer time intervals between injection and image acquisition, resulting in images with a higher target to background ratio, but the disadvantage of iodine as a radiolabel is the rapid dehalogenation, slow plasma clearance of the tracer, and the higher radiation dose to the body, compared to the short-lived radioisotopes carbon-11 and fluorine-18. In addition, the short half-life of ^{11}C and ^{18}F (20 min and 110 min, respectively) allows for sequential PET imaging in the same animal or human.^{4–6}

All of the acyclo-guanosine derivatives for PET have used fluorine-18 as a radiolabel.^{4,7–9} Of all the tracers evaluated, 2'-deoxy-2'-[^{18}F]fluoro-5-fluoro-1- β -D-arabinofuranosyluracil (^{18}F -FFAU) appears to be the most sensitive,⁹ while 9-(4-[^{18}F]fluoro-3-hydroxymethylbutyl)guanine (^{18}F -FHBG) is the most extensively studied PET reporter probe for imaging HSV1-tk gene expression.^{10,11} The advantages and disadvantages of these different radiolabeled probes have been compared and extensively discussed in literature.^{4,9} Other PET reporter genes that are identified and studied include human dopamine 2 receptor (hD₂R) gene, the human somatostatin receptor subtype-2 (hSSTR2), and human sodium iodide symporter (hNIS) transporter genes. To date, however, the majority of applications of

* Corresponding author: Herestraat 49 bus 821, BE 3000 Leuven, Belgium. Tel +32 16 330447. Fax: +32 16 330449. E-mail: guy.bormans@pharm.kuleuven.be.

[†] Laboratory for Radiopharmacy.

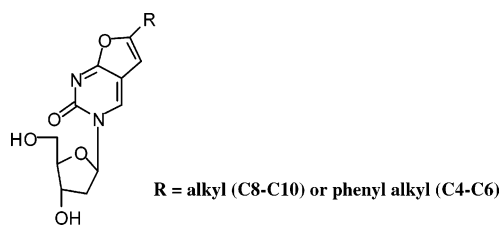
[‡] Department of Nuclear Medicine.

[§] Rega Institute for Medical Research.

^{||} Division of Molecular Medicine.

^a Abbreviations: VZV, varicella-zoster virus; tk, thymidine kinase gene; TK, thymidine kinase enzyme; BCNAs, bicyclic nucleoside analogues; HSV1, herpes simplex virus type 1; PET, positron emission tomography; ^{18}F -FHBG, 9-(4-[^{18}F]fluoro-3-hydroxymethylbutyl)guanine; BBB, blood-brain barrier; Clog*P*, calculated log partition coefficient; CC₅₀, 50% cytostatic concentration; 293T cells, human embryonic kidney cells; DMF, dimethylformamide; RP-HPLC, reversed phase high performance liquid chromatography; HRMS, high-resolution mass spectrometry; ^{18}F FEtBr, ^{18}F fluoroethyl bromide; ^{11}C MeI, ^{11}C methyl iodide; Ci, curie; IC₅₀, 50% inhibitory concentration; OST, osteosarcoma; % ID, % of injected dose; p.i., post injection; SUV, standard uptake value; LV, lentiviral vector; EMCV IRES, encephalomyocarditis virus internal ribosome entry sequence; LV-VZVTK-I-P, lentiviral vector encoding the VZV-tk gene and a puromycin resistance gene (*pac*, puromycin-N-acetyl-transferase); LV-LacZ-I-P, lentiviral vector encoding the LacZ gene and a puromycin resistance gene (*pac*, puromycin-N-acetyl-transferase); NaI(Tl), thallium doped sodium iodide; ES, electrospray ionization; EOS, end of synthesis; EtOH, ethanol; *t_R*, retention time; dThd, deoxythymidine; PBS, phosphate-buffered saline

Chart 1



radionuclide-based PET reporter gene/reporter probe technologies have used HSV1-tk reporter gene.¹²

In addition to monitoring gene expression in gene therapy models, PET reporter gene/reporter probe system can also be used for noninvasive imaging of stem cell trafficking. The exceptional regenerative capacity of stem cells encouraged scientists to explore the development of novel treatment for a wide variety of human diseases, including Parkinson's disease, Alzheimer's disease, and stroke. The ability of PET reporter genes to stably transfect into these cell populations prior to systemic administration provides a means to repetitively monitor the location of engrafted cells, their expansion, and the longevity of the transplant in treating these diseases, in brain.^{12,13} However, to monitor gene expression in the brain, either in gene therapy models or for cell tracking, lipophilic tracers that can cross the blood brain-barrier (BBB) are required. In order for a compound to be able to pass through BBB, its log partition coefficient (log*P*) value should ideally be in the range 0.5 to 2.5, its molecular mass should be less than 650 Da, and it should be uncharged.^{14,15} Unfortunately, however, none of the up-to-now developed PET reporter probes for the widely used HSV1-tk reporter gene is able to cross the BBB efficiently, probably due to their hydrophilic nature (log*P* value <0.5).^{4,16} As a result, the HSV1-tk reporter gene system is restricted to applications outside the brain only. For this reason and also because of the usefulness of monitoring different molecular events by imaging the expression of different genes in the same animal, there is a high demand for new PET-reporter systems.

Recently, a new class of antiviral compounds called bicyclic furoimidine deoxynucleoside analogues (BCNAs) was developed by McGuigan et al.¹⁷ These compounds are highly potent and selective inhibitors of VZV replication, and a critical requirement for the anti-VZV activity is the presence of a long alkyl or alkyl-aryl side chain at the 6-position of the furo ring (Chart 1). They display high lipophilicity values, as could be anticipated from their long alkyl side chains, with calculated log*P* (Clog*P*) values ranging between 0.4 and 4.6. Cytotoxicity of these agents in cell cultures was noted at high concentrations only (CC₅₀ ≥ 200 μM), giving them a very high selectivity index (SI > 5000). The absence of activity against thymidine kinase-deficient VZV strains implies an absolute need for a VZV TK-mediated phosphorylation to the corresponding 5'-monophosphates as a prerequisite for their antiviral action.¹⁸ Experiments using purified VZV TK and HSV-1 TK show that the BCNAs are phosphorylated by VZV TK but are not a substrate for HSV-1 TK.¹⁹ In addition, the thymidylate (dTMP) kinase activity of VZV-tk gene further converts the BCNA monophosphate (BCNA-5'-MP) to a BCNA diphosphate (BCNA-5'-DP).¹⁹ So far, no BCNA triphosphate formation has been detected in *in vitro* enzymatic assays and cell systems. The BCNAs (or their phosphorylated derivatives) are not a substrate for mammalian cytosolic TK-1, mitochondrial TK-2, or cytosolic dTMP kinase.¹⁹

These data suggest that a BCNA labeled with a positron emitting radioisotope might be selectively phosphorylated and

trapped in cells that express VZV-tk gene, and this might allow *in vivo* visualization of these cells using PET. This will not only result in a new PET reporter gene/probe system but may also allow the design of a BCNA that is able to pass the BBB, as suggested by the high Clog*P* values of this class of compounds. In addition, the high VZV specificity of these molecules, which makes them unique among nucleoside antivirals, may potentially allow the visualization of varicella-zoster infection in patients. Although *n*-C4–C6 alkylphenyl-BCNAs have a higher antiviral potency, we chose to synthesize BCNAs with chain length C1–C2 in view of their high VZV TK affinity,²⁰ which is a more predictive parameter for the potential use of BCNAs as VZV-tk visualization probes. We further aimed to develop BCNA-based PET reporter probes able to cross the BBB. As phenols can be efficiently methylated or fluoroethylated using ^{12/11}CH₃I or ^{19/18}FCH₂CH₂Br, respectively, we chose to synthesize the methoxy- and fluoroethoxyalkylphenyl-BCNAs (**3** and **2**) using the phenol **1** as a precursor.

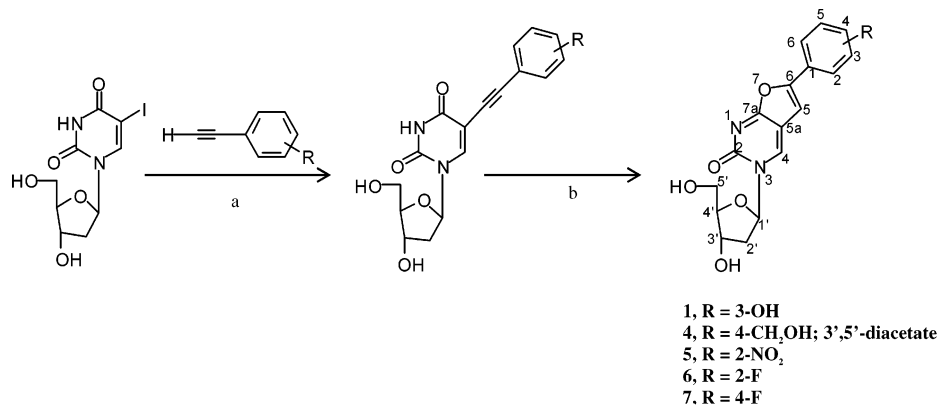
Herein this study we report the synthesis of stable and radiolabeled BCNAs **2** and **3**, their *in vitro* affinity for VZV TK, their biodistribution in normal mice, and the study of the *in vivo* stability of [¹¹C]-**3**. Finally, a cell uptake study was carried out in VZV-tk expressing human embryonic kidney (293T) cells.

Results and Discussion

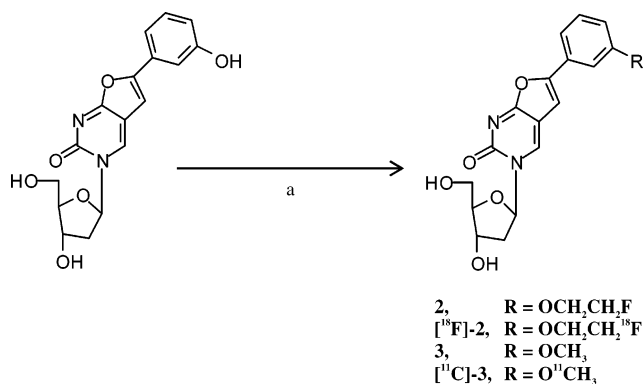
Chemistry. The phenolic precursor compound **1** was synthesized following the procedure described by McGuigan et al.²¹ which involved a Sonogashira coupling of 3-hydroxyphenyl acetylene to 5-iodo-2'-deoxyuridine under cocatalysis of Pd and cuprous ions. The resulting uncyclized intermediate was then cyclized *in situ* by treatment with cuprous iodide in triethylamine and methanol at reflux to obtain the fluorescent compound **1** in moderate yield (Scheme 1). To obtain pure compound **1**, the crude reaction mixture was first purified using silica gel column chromatography, and the isolated product was treated with hot acetonitrile to extract lipophilic impurities. The compound **1** was identified using mass spectrometry and characterized using NMR. The absence of a NH proton that usually occurs at 11.5 ppm for uridine derivatives¹⁷ and the presence of the C-5 proton as a sharp singlet (δ_H 7.2) in the ¹H NMR spectrum strongly support the hypothesis that the compound is cyclized.

Compound **1** was used as precursor for chemical and radiochemical synthesis of **2** and **3**. Alkylation of the phenol was achieved in good yields by heating with fluoroethyl bromide or methyl iodide in the presence of potassium carbonate as base (Scheme 2). Synthesis of the nonradioactive compounds was monitored using TLC, where the products appeared as highly fluorescent spots (**2**, *R_f* = 0.83; **3**, *R_f* = 0.8), and was followed by purification using preparative RP-HPLC. The ¹H NMR spectrum of the fluoroethyl derivative **2** showed the appearance of multiplets between 4.27 and 4.91 ppm, consistent with the presence of CH₂CH₂F, with a characteristic ²J_{H-F} coupling of 48 Hz and a ³J_{H-F} coupling of 26.9 Hz. The spectrum of the methyl ether **3** showed a sharp singlet at 3.83 ppm, corresponding to OCH₃ protons. Compounds **4–7** were also prepared following the same procedure as **1**. High-resolution mass spectrometry (HRMS) yielded the exact mass as calculated, for all the compounds (**1–7**).

Radiochemistry. Several attempts to label the BCNAs with fluorine-18 by reaction of a suitable precursor with [¹⁸F]fluoride failed due to a number of difficulties. As an example, we were unsuccessful in transforming the hydroxyl group of a *p*-hydroxymethyl derivative **4** into a tosylate or a nosylate.

Scheme 1. Synthesis of Precursors for Radiolabeling and Some of the Reference Fluorinated Compounds^a

^a Reagents and conditions: (a) Pd(PPh₃)₄, iPr₂EtN, CuI, DMF, RT, 19 h (b) Et₃N/MeOH, CuI, reflux, 4 h.

Scheme 2. Synthesis of Nonradioactive and Radiolabeled Compounds **2** and **3**^a

^a Reagents and conditions: (a) BrCH₂CH₂^{19/18F/12/11}CH₃I, DMF, base, Δ.

Mesylation of **4** was achieved, but the product was very unstable, and moreover, exposing compound **4** to radiolabeling conditions (heating at 110 °C for 10 min in the presence of K₂CO₃ and Kryptofix 222) resulted in extensive decomposition. An attempt to label the 2-nitro derivative **5** using an aromatic nucleophilic substitution with [¹⁸F]fluoride also failed and resulted in decomposition of the precursor. These failures prompted us to consider the use of secondary labeling agents, namely [¹⁸F]fluoroethyl bromide ([¹⁸F]FETBr) and [¹¹C]methyl iodide ([¹¹C]MeI). [¹⁸F]FETBr and [¹¹C]MeI were synthesized following reported procedures^{22,23} with some modifications. DMF was chosen as solvent because of the higher solubility of the compounds and the formation of less side products than in ethanol. Cesium carbonate (Cs₂CO₃) was used as base for radiosynthesis of both tracers, because of its better solubility in the organic solvent than K₂CO₃ and a faster alkylation rate. [¹⁸F]-**2** was synthesized by heating the radiolabeling precursor **1** with [¹⁸F]FETBr in DMF in the presence of 0.5–0.8 mg of Cs₂CO₃ at 90 °C for 15 min. Similarly, [¹¹C]-**3** was prepared by heating the precursor **1** with [¹¹C]MeI in DMF in the presence of 0.5–0.8 mg of Cs₂CO₃ at 90 °C for 10 min. For both the tracers, the synthesis was followed by evaporation at 50 °C of the unreacted labeling reagent with a sweep of helium gas and subsequent purification using preparative RP-HPLC. This evaporation of unreacted labeling reagent was useful for an efficient purification, particularly for [¹⁸F]-**2**, as unreacted [¹⁸F]-FETBr eluted just after [¹⁸F]-**2** on RP-HPLC. Chemical and radiochemical purity of both HPLC purified tracers was examined on analytical RP C₁₈ column and were always found to be >99%. The identity of the tracers was confirmed by

coelution with authentic nonradioactive compounds after coinjection on analytical RP-HPLC, employing 30% acetonitrile in 0.05 M sodium acetate buffer (pH 5.5) as mobile phase at 1 mL flow rate (Figure 1; [¹⁸F]-**2**, *t*_R = 8.1 min; [¹¹C]-**3**, *t*_R = 7.0 min).

Partition Coefficient. The lipophilicity of the RP-HPLC purified radiolabeled products was determined by partitioning between 1-octanol and 0.025 M phosphate buffer pH 7.4 (*n* = 6). The log partition coefficient values of [¹⁸F]-**2** and [¹¹C]-**3** were 1.24 and 1.27, respectively, and are within the optimal range for passive diffusion of a compound through the BBB.¹⁴

Affinity and Cytostatic Activity of the Compounds. The test (nonradioactive) compounds were evaluated for their affinity for purified recombinant VZV TK, HSV-1 TK, and human cytosolic TK-1, and the results are expressed as 50% inhibitory concentration (IC₅₀) values. The phenolic precursor **1** and its *O*-methyl derivative **3** exhibited good affinity for VZV TK with IC₅₀ values 2.6 μM and 4.8 μM, respectively, whereas the fluoroethyl derivative **2** has only moderate affinity (Table 1). These values are comparable to those of *n*-alkylphenyl-BCNAs that have very high antiviral activity²⁰ and may indicate that the affinity of such compounds (**1–3**) for VZV TK decreases as the alkyl chain length increases, and/or that the presence of a fluorine atom compromises the affinity for the enzyme. Compounds **6** and **7** were synthesized with the intention to be used as reference substances for radiolabeled products synthesized from corresponding nitro precursors. In affinity tests, the fluoro derivatives **6** and **7** showed high affinity for VZV TK with IC₅₀ values around 0.2 μM (Table 1). In fact, of all the compounds synthesized and examined in this work, these two compounds have the highest affinity for the enzyme. In contrast to their affinity for VZV TK, the test compounds are not activated (phosphorylated) by other nucleoside kinases examined (HSV-1 TK, cytosolic TK-1), with IC₅₀ values > 500 μM (Table 1). Our observation confirms the previous findings²⁰ and provides the basis for explaining the specificity of these compounds for VZV TK.

The cytostatic activity of BCNA compounds **1–3** was also examined using osteosarcoma (OST) cells and expressed as the 50% cytostatic concentration (CC₅₀). For comparison, the CC₅₀ of penciclovir and its fluorinated analogue (FHBG) was also determined. No cytotoxicity was observed for compounds **1**, **2**, and **3** in control as well as HSV-1 TK- and VZV TK-expressing OST cells (data not shown), contrary to penciclovir and its fluorinated analogue (FHBG), which are cytostatic against OST TK⁻/HSV-1 TK⁺ cells at 0.038 μM and 1.8 μM, respectively. The anti-proliferative activity of penciclovir and FHBG can be

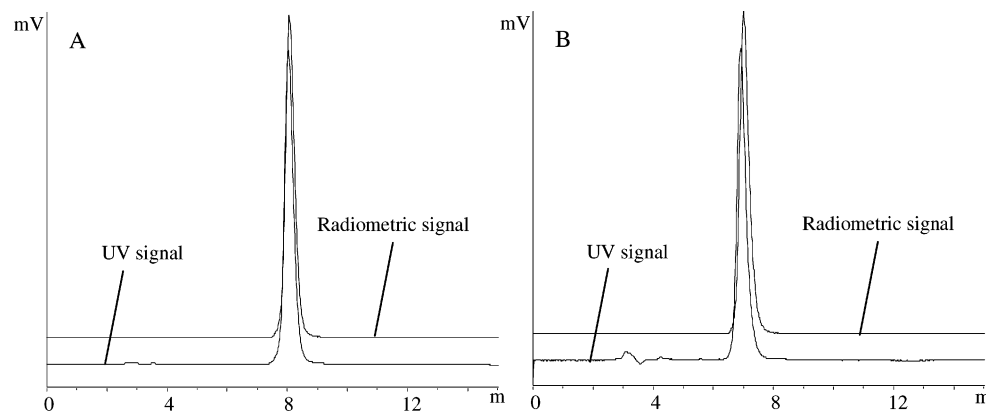


Figure 1. Quality control HPLC chromatograms of [^{18}F]-**2** (A; $t_R = 8.1$ min) and [^{11}C]-**3** (B; $t_R = 7.0$ min) coinjected with authentic nonradioactive compounds. Stationary phase: XTerra RP C_{18} ($5 \mu\text{m}$, $4.6 \text{ mm} \times 250 \text{ mm}$); Mobile phase: 0.05 M sodium acetate (pH 5.5)/acetonitrile (70:30); Flow rate: 1 mL/min; Detection: UV 254 nm.

Table 1. Affinity of the Synthesized Nonradioactive Compounds for the Enzymes VZV TK, HSV-1 TK, and Cytosolic TK-1

compound	R	IC_{50}^a (μM)		
		VZV TK	HSV-1 TK	cytosolic TK-1
1	OH	2.6 ± 0.1	>500	>500
2	$\text{OCH}_2\text{CH}_2\text{F}$	53 ± 12	>500	>500
3	OCH_3	4.8 ± 1.7	>500	>500
6	2-F	0.28 ± 0.1	>500	>500
7	4-F	0.18 ± 0.1	>500	>500
penciclovir	-	>50	11 ± 0	-
FHBG	-	>50	9 ± 4.2	-

^a 50% inhibitory concentration or compound concentration required to inhibit nucleoside kinase-catalyzed phosphorylation of $1 \mu\text{M}$ [$\text{CH}_3\text{-}^3\text{H}$]dThd by 50%.

Table 2. Biodistribution of [^{18}F]-**2** in Normal Mice at 2 and 60 min p.i. (data are expressed as mean \pm SD; $n = 3$ per time point)

organ	%ID ^a		SUV ^b	
	2 min	60 min	2 min	60 min
urine	5.7 ± 1.3	29.5 ± 9.4	-	-
kidneys	15.5 ± 5.8	1.2 ± 1.0	9.0 ± 3.3	0.7 ± 0.6
liver	24.4 ± 3.8	4.4 ± 1.5	3.9 ± 0.8	0.7 ± 0.2
spleen + pancreas	1.3 ± 0.2	0.1 ± 0.1	1.4 ± 0.1	0.1 ± 0.1
lungs	0.9 ± 0.1	0.1 ± 0.0	1.1 ± 0.2	0.0 ± 0.0
heart	0.3 ± 0.0	0.0 ± 0.0	0.6 ± 0.1	0.0 ± 0.0
intestines	20.7 ± 4.4	60.5 ± 7.9	-	-
brain	0.0 ± 0.0	0.0 ± 0.0	0.1 ± 0.0	0.0 ± 0.0
blood	6.2 ± 1.0	0.4 ± 0.1	0.9 ± 0.1	0.1 ± 0.0
carcass	27.2 ± 3.3	3.8 ± 0.3	-	-

^a Percentage of injected dose calculated as cpm in organ/total cpm recovered. ^b Standard uptake values calculated as (radioactivity in cpm in organ/weight of the organ)/(total counts recovered/body weight).

attributed to their phosphorylation by HSV-1 TK, resulting in the eventual formation of cytotoxic phosphorylated metabolites, whereas this is not the case with BCNAs because they do not have any affinity for HSV-1 TK. Also, since the BCNAs are not cytostatic to VZV-tk gene-transduced OST TK⁻ cells (data not shown), this suggests that the phosphorylated BCNA metabolites does not have affinity for cellular enzymes in order to be converted to potential cytotoxic metabolites.

Biodistribution and Biostability in Normal Mice. The results of in vivo biodistribution studies of the radiolabeled tracers [^{18}F]-**2** and [^{11}C]-**3** in NMRI mice show that they behave similarly (Tables 2 and 3). Blood clearance was very rapid for both tracers (<0.5% of injected dose (ID) in blood at 60 min postinjection (p.i.)). As could be expected from their $\log P$ values, the compounds were cleared mainly by the hepatobiliary system ([^{18}F]-**2** 60.5% and [^{11}C]-**3** 63.7% of ID in intestines at 60 min p.i.) and to a lesser extent to the urine ([^{18}F]-**2** 29.5%

Table 3. Biodistribution of [^{11}C]-**3** in Normal Mice at 2 and 60 min p.i. (data are expressed as mean \pm SD; $n = 3$ per time point)

organ	%ID ^a		SUV ^b	
	2 min	60 min	2 min	60 min
urine	0.2 ± 0.1	28.2 ± 3.0	-	-
kidneys	21.7 ± 3.1	0.3 ± 0.1	12.4 ± 0.9	0.2 ± 0.0
liver	21.3 ± 3.6	3.7 ± 2.3	3.7 ± 0.9	0.7 ± 0.4
spleen + pancreas	2.4 ± 0.2	0.1 ± 0.0	2.7 ± 0.0	0.1 ± 0.0
lungs	0.7 ± 0.1	0.0 ± 0.0	1.0 ± 0.1	0.0 ± 0.0
heart	0.5 ± 0.1	0.0 ± 0.0	1.0 ± 0.2	0.0 ± 0.0
intestines	25.6 ± 4.1	63.7 ± 3.4	-	-
brain	0.0 ± 0.0	0.0 ± 0.0	0.1 ± 0.0	0.0 ± 0.0
blood	5.4 ± 0.6	0.2 ± 0.0	0.8 ± 0.1	0.0 ± 0.0
carcass	25.3 ± 2.2	3.5 ± 1.1	-	-

^a Percentage of injected dose calculated as cpm in organ/total cpm recovered. ^b Standard uptake values calculated as (radioactivity in cpm in organ/weight of the organ)/(total counts recovered/body weight).

and [^{11}C]-**3** 28.2% of ID in urine at 60 min p.i.). Except for liver (3.7–4.4% ID) and intestines (60–64% ID), the radioactivity in other major organs was negligible after 60 min for both tracers. At 2 min p.i. the highest concentration of radioactivity was found in the kidneys with a standard uptake value (SUV) of 9.0 ± 3.3 for [^{18}F]-**2** and 12.4 ± 0.9 for [^{11}C]-**3**. This was succeeded by liver with SUV values around 3.8, for both tracers. At 60 min p.i., these values were 0.7 or less for all the organs, indicating good clearance of the tracers. For successful imaging of VZV-tk gene expression in brain, brain penetration of BCNA tracers is a prerequisite, followed by their phosphorylation by the protein product of VZV-tk gene and subsequent entrapment in the cells. As described above, for a reasonable uptake in the brain, the $\log P$ value of a compound should be between 0.5 and 2.5 and its molecular mass should be less than 650 Da and be uncharged.^{14,15} The $\log P$ of [^{18}F]-**2** is 1.24 and that of [^{11}C]-**3** is 1.27, both compounds are uncharged at physiological pH, and their molecular mass is 413 and 381 Da, respectively. However, negligible brain uptake was observed for both probes albeit the above-mentioned requirements for the brain uptake are fulfilled. This implies that besides the general requirements of lipophilicity, molecular mass, and charge, other factors or properties of the molecule do influence BBB penetration. It is hypothesized that the presence of the polar sugar moiety might be detrimental for BBB penetration of these tracers, and work is in progress to evaluate this hypothesis by studying the brain uptake of the corresponding compounds in which the sugar hydroxyl groups are esterified, although these derivatives are anticipated not to have affinity for VZV TK. Hence, the synthesized tracers ([^{18}F]-**2** and [^{11}C]-**3**) can be useful for

Table 4. In Vitro Incorporation of [¹⁸F]-**2** and [¹¹C]-**3** in VZV-tk Gene- and LacZ Gene-Transduced 293T Cells at Time of Maximal Uptake (3 and 1 h, respectively)

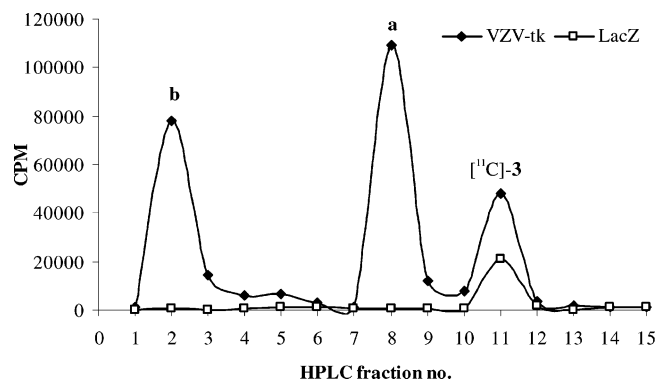
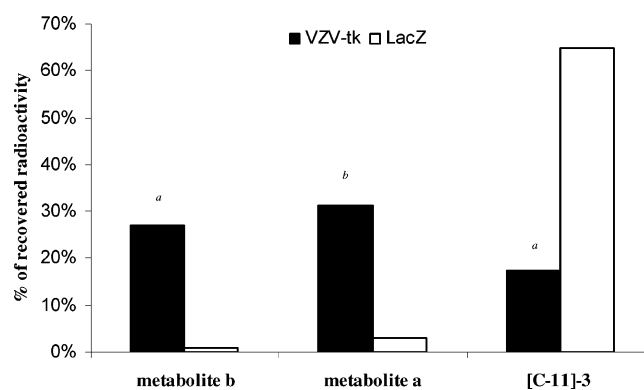
expt	compd	radioactivity in LV-VZVTK-I-P transduced cells ^a	radioactivity in LV-LacZ-I-P transduced cells ^a	uptake ratio	average ratio ^b
1	[¹⁸ F]- 2	2.55	0.47	5.4	4.5 ± 0.8
2		2.04	0.47	4.3	
3		2.29	0.60	3.8	
1	[¹¹ C]- 3	12.80	0.24	53.8	53 ± 1.2
2		11.55	0.22	53.6	
3		12.26	0.24	51.6	

^a Data are expressed as % tracer/mg protein. ^b Data are expressed as mean ± SD, *p* < 0.0005.

imaging varicella-zoster virus infection as well as VZV-tk reporter gene expression in vivo outside the brain only.

In vivo stability of [¹¹C]-**3** after intravenous (i.v.) injection in normal mice was assessed by RP-HPLC analysis of plasma and urine. For this purpose a novel Oasis HLB column containing reversed phase sorbent was employed.²⁴ After injection of the samples on to Oasis column, the proteins and other hydrophilic matrix components were washed from the column using HPLC grade water. The analytes were then eluted from the Oasis column and led over an RP-analytical column, the eluate of which was collected in 1-mL fractions followed by counting of all the fractions for radioactivity. At 2 min p.i. of [¹¹C]-**3**, 98% of the recovered radioactivity was present as intact tracer in plasma, and this remained at a level of 80% at 30 min p.i. Urine analysis at 30 and 60 min after injection of [¹¹C]-**3** showed that 90–93% of the recovered radioactivity was the parent tracer. This also confirms a negligible metabolism of the tracer, especially to polar compounds that are excreted via the urine. BCNAs were found to be highly stable compounds in vivo. Indeed, they are not susceptible to breakdown by the nucleoside catabolic enzyme thymidine phosphorylase, which converts many pyrimidine nucleosides into the inactive free base as shown before.^{25,26} On the basis of these data, metabolism of [¹⁸F]-**2** and [¹¹C]-**3** to their free bases in plasma is highly unlikely.

In Vitro Evaluation of the Tracers. In vitro evaluation of [¹⁸F]-**2** and [¹¹C]-**3** was performed in 293T cell (human embryonic kidney) cultures, transduced with lentiviral vector (LV) encoding the VZV-tk gene or the LacZ gene (control) and a puromycin resistance gene (*pac*, puromycin-*N*-acetyl-transferase) linked by the encephalomyocarditis virus internal ribosome entry (EMCV IRES) sequence. The LV were produced and cell cultures were transduced as described earlier.²⁷ Cell lines were denominated LV-VZVTK-I-P or LV-LacZ-I-P and incubated with [¹⁸F]-**2** or [¹¹C]-**3** at 37 °C for different time intervals. It was found that a maximal uptake was observed after 3 h incubation for [¹⁸F]-**2** and 1 h incubation for [¹¹C]-**3**. Further evaluation of cell uptake was done at the respective time of maximal uptake. As shown in Table 4, uptake of [¹⁸F]-**2** and [¹¹C]-**3** in the LV-VZVTK-I-P cells was 4.5- and 53-fold higher, respectively, than in control cells (*n* = 3; *p* < 0.0005 for both, unpaired bidirectional Student *t*-test). The affinity of compound **3** for VZV TK is about 11-fold higher compared to compound **2** (see Table 1), and this is clearly reflected in the results of the cell uptake experiments using the radiolabeled tracers. Indeed, the uptake ratio of [¹¹C]-**3** was about 12-fold higher than that of [¹⁸F]-**2**. This accumulation of [¹⁸F]-**2** and [¹¹C]-**3** into LV-VZVTK-I-P-transduced cells suggests their specific phosphorylation by the VZV TK enzyme present in these cells. BCNAs do not have affinity for closely related HSV-1 TK and for human cytosolic TK-1 and mitochondrial TK-2, and the lack of

**Figure 2.** RP-HPLC radiochromatogram of [¹¹C]-**3** and its metabolites (**a** & **b**) from the cell lysate of VZV-tk gene- and LacZ gene-transduced 293T cells, after 30 min incubation. Stationary phase: Oasis HLB (4.6 mm × 20 mm), XTerra RP C₁₈ (5 μm, 4.6 mm × 250 mm); Mobile phase: 0.05 M ammonium acetate/acetonitrile (70:30); Flow rate: 1 mL/min; Detection: UV 254 nm.**Figure 3.** Metabolism of [¹¹C]-**3** in VZV-tk gene- and LacZ gene-transduced 293T cells after 30 min incubation. Data are the average of two independent experiments; ^a *p* < 0.005, ^b *p* < 0.05.

accumulation of [¹⁸F]-**2** and [¹¹C]-**3** by LV-LacZ-I-P-transduced cells in these experiments further confirm their specificity for VZV TK. The specificity of these tracers for VZV TK will allow to monitor VZV-tk gene expression even in the presence of other reporter genes like HSV1-tk and LacZ.

To check the nature of the metabolites trapped in the LV-VZVTK-I-P-transduced cells, the cell lysate after incubation with [¹¹C]-**3** was analyzed using RP-HPLC, similar to the in vivo stability analysis. As expected, the recovered radioactivity was predominant among two additional hydrophilic components, besides residual parent tracer (Figure 2). The first component was not retained on the Oasis column and eluted with the first 3 mL water rinse (fraction no. 2). The second component eluted between 4 and 5 min (fraction no. 8), while the parent tracer eluted at 8.5 min (in fraction no. 11). On the basis of reported data on phosphorylation of BCNAs,¹⁹ we assume that the first compound (metabolite b) is the diphosphorylated derivative and the second the monophosphorylated metabolite (metabolite a), estimated as 27% and 31% of recovered radioactivity, respectively (Figure 3). Since unlabeled phosphate derivatives of compound **3** are not available, our structure assignment is tentative, and further studies are necessary for the precise identification of these metabolic species. Analysis of the cell lysate from LV-LacZ-I-P-transduced cells showed no significant presence of metabolite a or b, and the majority of the recovered radioactivity corresponds to the parent tracer (Figure 3).

Conclusion

An efficient and convenient chemical and radiochemical synthesis of a novel class of bicyclic nucleoside analogues ([¹⁸F]-**2** and [¹¹C]-**3**) was developed. In vitro affinity of precursor **1** and methyl ether **3** for VZV TK was pronounced, while the affinity of **2** was moderate. The radiochemical synthesis produced [¹⁸F]-**2** and [¹¹C]-**3** in amounts and purity suitable for PET studies. To our knowledge this is the first report on radiolabeling of BCNAs. Cell uptake studies revealed that [¹¹C]-**3** accumulates to a higher degree (~12-fold) compared to [¹⁸F]-**2** in VZV-tk expressing cells than in LacZ expressing (control) cells. RP-HPLC analysis of cell lysate from the VZV-tk expressing cell line at 30 min after incubation with [¹¹C]-**3** showed the presence of two hydrophilic components, presumably its mono- and diphosphorylated form. The metabolic stability analysis revealed that 80% of the tracer was left unchanged in plasma after 30 min after injection of [¹¹C]-**3** in mice, and this remained at 90% in urine sample at 60 min postinjection. The objective of this work was to synthesize radiolabeled BCNAs that can cross the BBB for monitoring VZV-tk gene expression in the brain using PET. Despite favorable physical properties for BBB passage, the tracers did not show brain uptake in biodistribution studies in mice. Nevertheless, this study has resulted in a new PET reporter probe/gene system with a combination of labeled BCNA ([¹⁸F]-**2** or [¹¹C]-**3**) as reporter probe and VZV-tk as reporter gene. We conclude that this new PET reporter probe/gene system can be useful for monitoring VZV-tk gene expression in the body other than the brain, and even in the presence of other reporter genes such as HSV1-tk and LacZ. Since [¹¹C]-**3** has shown high affinity for VZV-tk in cell culture, further evaluation of this tracer is in progress in animal models expressing VZV-tk.

Experimental Section

Chemicals and Reagents. 3-Hydroxyphenylacetylene was obtained from Alfa Aesar KG (Karlsruhe, Germany). 1-Bromo-2-fluoroethane (FETBr) was purchased from ABCR RG (Im Schleiert, Germany). All other reagents and solvents were obtained commercially from Acros Organics (Geel, Belgium), Aldrich, Fluka, Sigma (Sigma-Aldrich, Bornem, Belgium), or Fischer Bioblock Scientific (Tournai, Belgium) and used as supplied.

Apparatus, Instruments, and General Conditions. All glassware was dried in an oven at 110 °C for several hours and allowed to cool to room temperature (RT) before use. For ascending thin layer chromatography (TLC), precoated aluminum backed plates (Silica gel 60 with fluorescent indicator, 0.2 mm thickness; supplied by Macherey-Nagel (Düren, Germany) were used and developed using 10% CH₃OH in CH₂Cl₂ as mobile phase for all the compounds. After evaporation of the solvent, compounds were detected under UV light (254 or 366 nm). ¹H NMR spectra were recorded on a Gemini 200 MHz spectrometer (Varian, Palo Alto, CA) using DMSO-*d*₆ as solvent. Chemical shifts are reported in parts per million relative to TMS ($\delta = 0$). Coupling constants are reported in hertz (Hz). Splitting parameters are defined by s (singlet), d (doublet), dd (double doublet), t (triplet), and m (multiplet). HPLC purification and analysis was performed either on a Merck Hitachi L6200 intelligent pump (Hitachi, Tokyo, Japan) or on a Waters 600 pump (Waters Corporation, Milford, MA) connected to a UV spectrometer (Waters 2487 Dual λ absorbance detector) set at 254 nm. The output signal was recorded and analyzed using a RaChel data acquisition system (Lablogic, Sheffield, UK). For analysis of radiolabeled compounds, after passing through UV detector, the HPLC eluate was led over a 3 in. NaI(Tl) scintillation detector connected to a single channel analyzer (Medi-Lab Select, Mechlen, Belgium). The radioactivity measurements during biodistribution studies and cell-uptake studies were done using an automatic gamma counter (3 in. NaI(Tl) well

crystal) coupled to a multichannel analyzer (Wallac 1480 Wizard 3", Wallac, Turku, Finland). The values were corrected for background radiation and physical decay during counting. Exact mass measurement was performed on a time-of-flight mass spectrometer (LCT, Micromass, Manchester, UK) equipped with an orthogonal electrospray ionization (ESI) interface, operated in positive mode (ES+). Samples were infused in acetonitrile/water using a Harvard 22 syringe pump (Harvard Instruments, Holliston, MA). Accurate mass determination was done by coinfusion with a 10 μ g/mL solution of Kryptofix as an internal calibration standard. Acquisition and processing of data was done using Masslynx software (version 3.5, Waters). Melting points (MP) were determined using an IA9000 digital melting point apparatus (Electrothermal, Southend-on-Sea, England).

Syntheses. 3-(2'-Deoxy- β -D-ribofuranosyl)-6-(3-hydroxyphenyl)-2,3-dihydrofuro[2,3-*d*]pyrimidin-2-one (1). To a stirred solution of 5-iodo-2'-deoxyuridine (2.9 g, 8.19 mmol) in DMF (30 mL) under nitrogen at room temperature were added *N,N*-diisopropylethylamine (3.0 mL, 16.95 mmol), tetrakis(triphenylphosphine)palladium(0) (957 mg, 0.828 mmol), and copper(I) iodide (314 mg, 1.65 mmol), followed by the slow addition of a solution of 3-hydroxyphenylacetylene (2.9 g, 24.57 mmol) in 5 mL of DMF. The resulting mixture was stirred at room temperature (RT) for 19 h. After this time, TLC showed complete conversion of the starting material. Copper(I) iodide (290 mg), methanol (73 mL), and triethylamine (55 mL) were then added to the reaction mixture, which was heated under reflux for 4 h. The solvents were evaporated under reduced pressure, and the resulting residue was stirred with Amberlite IRA-400 (HCO₃⁻) in CH₃OH/CH₂Cl₂ (1:1) (20 mL) for 1 h. The resin was filtered and washed several times with methanol, and the combined filtrates were evaporated to dryness. The crude product was purified using column chromatography on silica gel eluted with gradient mixtures of CH₂Cl₂ and CH₃OH (up to 10%). Appropriate fractions were combined, and the solvent was removed under reduced pressure. Treating the resulting yellow residue with hot acetonitrile followed by filtration yielded the pure product as yellow crystals (1.1 g, 38%).

3-(2'-Deoxy- β -D-ribofuranosyl)-6-(3-fluoroethoxyphenyl)-2,3-dihydrofuro[2,3-*d*]pyrimidin-2-one (2). To a solution of **1** (40 mg, 0.116 mmol) in DMF (8 mL) were added K₂CO₃ (32.5 mg, 0.23 mmol) and dropwise a solution of 1-bromo-2-fluoroethane (22 μ L, 0.17 mmol in 2 mL of DMF). The reaction mixture was then stirred at 70 °C for 4 h after which a more lipophilic, highly fluorescent spot appeared on TLC. The product was purified by HPLC using a C-18 semipreparative column (PrepLC 25 mm module, Waters) eluted with 30% acetonitrile in water at a flow rate of 4 mL/min (*t*_R = 21 min). After evaporation of the solvent, the product was obtained as a white solid (44.5 mg, 98%).

3-(2'-Deoxy- β -D-ribofuranosyl)-6-(3-methoxyphenyl)-2,3-dihydrofuro[2,3-*d*]pyrimidin-2-one (3). To a solution of **1** (50 mg, 0.145 mmol) in DMF (8 mL) were added 41 mg (0.29 mmol) of K₂CO₃ and dropwise a solution of methyl iodide (31 μ L, 0.22 mmol in 2 mL of DMF). After being stirred at 70 °C for 4 h, the reaction mixture was purified by HPLC using a C-18 semipreparative column (PrepLC 25 mm module, Waters) eluted with 30% acetonitrile in water at a flow rate of 4 mL/min (*t*_R = 17.4 min). After evaporation of the solvent, the methylated product was obtained as a white solid (32 mg, 60%).

3-(2'-Deoxy- β -D-ribofuranosyl 3',5'-diacetate)-6-(4-hydroxymethyl-phenyl)-2,3-dihydrofuro[2,3-*d*]pyrimidin-2-one (4). The same procedure was used as described for compound **1**, but starting from 5'-iodo-2'-deoxyuridine 3',5'-diacetate (2.3 g, 5.25 mmol) and 4-ethynylbenzyl alcohol. The reaction mixture was purified three times by column chromatography using 0–6% CH₃OH in CH₂Cl₂ as mobile phase to yield the title compound as a white solid (520 mg, 20%).

3-(2'-Deoxy- β -D-ribofuranosyl)-6-(2-nitrophenyl)-2,3-dihydrofuro[2,3-*d*]pyrimidin-2-one (5). The same procedure was used as described for compound **1**, but using 2-nitrophenylacetylene instead of 3-hydroxyphenylacetylene. The compound was purified by column chromatography (6% MeOH in CH₂Cl₂) followed by

reversed phase medium-pressure LC (Knauer pump K-501, Knauer, Berlin, Germany) employing 25% acetonitrile in water as mobile phase at 6 mL/min flow rate to yield compound **5** as a yellow solid (150 mg, 14%).

3-(2'-Deoxy- β -D-ribofuranosyl)-6-(2-fluorophenyl)-2,3-dihydrofuro[2,3-*d*]pyrimidin-2-one (6**).** The same procedure was used as described for compound **1** but using 2-fluorophenylacetylene instead of 3-hydroxyphenylacetylene. The compound was purified by column chromatography (10% MeOH in CH₂Cl₂) to yield compound **6** as a white solid (400 mg, 41%).

3-(2'-Deoxy- β -D-ribofuranosyl)-6-(4-fluorophenyl)-2,3-dihydrofuro[2,3-*d*]pyrimidin-2-one (7**).** The same procedure was used as described for compound **1** but using 4-fluorophenylacetylene instead of 3-hydroxyphenylacetylene. The compound was purified by column chromatography (10% MeOH in CH₂Cl₂) to yield compound **7** as a white solid (480 mg, 49%).

Production of [¹⁸F]fluoride and Radiosynthesis of [¹⁸F]-2 Using [¹⁸F]FETBr. [¹⁸F]F⁻ was produced [¹⁸O(p, n)¹⁸F reaction] by irradiation of 0.5 mL of 97% enriched H₂¹⁸O (Rotem HYOX¹⁸, Rotem Industries, Beer Sheva, Israel) in a niobium target using 18-MeV protons from a Cyclone 18/9 cyclotron (Ion Beam Applications, Louvain-la-Neuve, Belgium) and separated from [¹⁸O]-H₂O using a SepPak Light Accell plus QMA anion exchange cartridge (Waters). The [¹⁸F]F⁻ was then eluted from the cartridge with a solution containing 2.47 mg of potassium carbonate and 27.92 mg of Kryptofix 222 dissolved in 0.75 mL of H₂O/CH₃CN (5:95) into a reaction vial.

After evaporation of the solvent from the reaction vial, [¹⁸F]F⁻ was further dried by azeotropic distillation of traces of water using acetonitrile. 2-Bromoethyl triflate (BrCH₂CH₂OTf) (5 μ L) in *o*-dichlorobenzene (0.7 mL) was added into the vial containing [¹⁸F]F⁻. The resulting [¹⁸F]FETBr was then distilled at 110 °C under a helium flow (3–4 mL/min) and bubbled into another reaction vial containing a solution of **2** (0.2 mg) and Cs₂CO₃ (0.5–0.8 mg) in anhydrous DMF (0.2 mL). After sufficient radioactivity was distilled into the solution, the reaction mixture was heated at 90 °C for 15 min. The unreacted [¹⁸F]FETBr was evaporated by flushing the mixture with helium at 50 °C until the radioactivity in the vial remained at a stable level. The crude mixture was then diluted with 1.6 mL of water and applied onto a HS HyperPrep RP C₁₈ 100 Å 8 μ m column (10 mm \times 250 mm; Alltech, Deerfield, IL) that was eluted with 0.05 M sodium acetate buffer (pH = 5.5)/EtOH (70:30) at a flow rate of 3 mL/min. The radiolabeled compound ([¹⁸F]-**2**) was collected at 18.4 min, whereas the precursor eluted at 8.4 min. The purity of the labeled tracer was analyzed using XTerra RP C₁₈ column (5 μ m, 4.6 mm \times 250 mm; Waters), eluted with 30% acetonitrile in 0.05 M sodium acetate buffer (pH 5.5) at a flow rate of 1 mL/min (*t*_R = 8.1 min). Decay corrected radiochemical yields were between 30 and 47%, with an average of 39 \pm 8% (relative to starting [¹⁸F]FETBr, *n* = 4). Starting from [¹⁸F]FETBr, the synthesis time to obtain the pure product was about 60 min. The average specific activity was found to be 1.94 Ci/ μ mol (71.8 GBq/ μ mol) at the end of synthesis (EOS).

Production of [¹¹C]MeI and Radiosynthesis of [¹¹C]-3. Carbon-11 was produced by a ¹⁴N(p, α)¹¹C nuclear reaction. The target gas (a mixture of 95% N₂ and 5% H₂) was irradiated using 18-MeV protons at a beam current of 25 μ A for about 25 min, to yield [¹¹C]CH₄. This was then reacted with vaporous I₂ at 650 °C to convert it to [¹¹C]MeI. The resulting volatile [¹¹C]MeI was bubbled into a reaction vial containing a solution of **3** (0.2 mg) and Cs₂CO₃ (0.5–0.8 mg) in anhydrous DMF (0.2 mL). When the radioactivity in the vial remained at a stable level, the reaction mixture was heated at 90 °C for 10 min. The unreacted [¹¹C]MeI was flushed from the reaction mixture by bubbling it with helium at 50 °C for about 1 min. The crude reaction mixture was diluted with water and purified in the same manner as for [¹⁸F]-**2**, except that 35% EtOH was used in the mobile phase (*t*_R = 13 min). The purity of the labeled tracer was analyzed using XTerra RP C₁₈ column (5 μ m, 4.6 mm \times 250 mm; Waters), eluted with 30% acetonitrile in 0.05 M sodium acetate buffer (pH 5.5) at a flow rate of 1 mL/min (*t*_R = 7.0 min). [¹¹C]-**3** was synthesized in about

51 \pm 13% yield (relative to starting [¹¹C]MeI, non-decay-corrected, *n* = 3), and the specific radioactivity was between 1.38 and 2.14 Ci/ μ mol (51.1–79.3 GBq/ μ mol), at EOS.

Partition Coefficient Determination. An aliquot of 25 μ L of RP-HPLC isolated labeled product containing 5 μ Ci of [¹⁸F]-**2** or 15 μ Ci of [¹¹C]-**3** was added to a tube containing a mixture of 1-octanol and 0.025 M phosphate buffer pH 7.4 (2 mL each). The test tube was vortexed at room temperature for 2 min followed by centrifugation at 3000 rpm (1837g) for 5 min (Eppendorf centrifuge 5810, Eppendorf, Westbury, NY). Aliquots of 61 and 500 μ L were drawn from the 1-octanol and aqueous phases, respectively, taking care to avoid cross-contamination between the two phases. The radioactivity in the aliquots was counted using an automatic gamma counter. After correction for the density and the mass difference between the two phases, the partition coefficient (*P*) was calculated as (radioactivity (cpm) in 1-octanol)/(radioactivity (cpm) in phosphate buffer pH 7.4).

Biodistribution in Normal Mice. Solutions of [¹⁸F]-**2** and [¹¹C]-**3** obtained after RP-HPLC purification were diluted using water for injection to a concentration of 0.1 mCi/mL and 1 mCi/mL, respectively. The biodistribution of both tracers was determined in male NMRI mice (weight 30–40 g). The animal studies were performed according to the Belgian code of practice for the care and use of animals, after approval from the university ethics committee for animals. A volume of 0.1 mL of the diluted tracer solution was injected into the mice via a tail vein, under anesthesia (intraperitoneal injection of 0.1 mL of a solution containing 3 mg of ketamine and 0.225 mg of xylazine). The mice were sacrificed by decapitation at 2 or 60 min after injection (*n* = 3 at each time point). Blood was collected in a tared tube and weighed. All organs and other body parts were dissected and weighed, and their radioactivity was counted in a gamma counter. Results are expressed as %ID (cpm in organ/total cpm recovered), or, where possible, as SUVs. SUVs were calculated as (radioactivity in cpm in organ/weight of the organ)/(total counts recovered/body weight). For calculation of total radioactivity in blood, blood mass was assumed to be 7% of the body mass.²⁸

Metabolism of [¹¹C]-3 in Mice. The metabolic stability of [¹¹C]-**3** was studied in normal mice by determination of the relative amounts of the parent tracer and metabolites in blood and urine. After intravenous administration of 0.35–0.4 mCi of [¹¹C]-**3** into mice, the animals were sacrificed by decapitation at 2 or 30 min p.i. (one mouse per time point). Blood was collected into a BD vacutainer (containing 7.2 mg K₂EDTA; BD, Franklin Lakes, NJ) and subsequently transferred to a 1.5-mL eppendorf tube. The samples were then centrifuged at 3000 rpm (1837g) for 5 min (Eppendorf centrifuge 5810, Eppendorf), to separate plasma. The supernatant plasma sample was mixed with 25 μ L of authentic **3** (0.5 mg/1.5 mL) and injected onto an Oasis HLB column (hydrophilic–lipophilic balanced; 4.6 mm \times 20 mm, Waters) that was preconditioned by successive washings with acetonitrile and water. The eluate from the Oasis column was collected (fraction 1). The proteins of the biological matrix were washed from the Oasis column with 6 mL of water, which was collected as two 3-mL fractions (fraction no. 2 and 3). The outlet of the Oasis column was then connected to a XTerra RP C₁₈ column (5 μ m, 4.6 mm \times 250 mm; Waters), and both columns in series were then eluted using 0.05 M ammonium acetate/acetonitrile (70:30) as the mobile phase at a flow rate of 1 mL/min. After being passed through an in-line UV detector, the HPLC eluate was collected in 1-mL fractions and their radioactivity as well as the activity in fractions 1–3 was measured using a gamma counter. Urine samples were collected from mice sacrificed at 30 or 60 min p.i., mixed with authentic **3**, and analyzed following the same procedure, without any pretreatment or workup.

Affinity of Test Compounds for Nucleoside Kinase Enzymes in Vitro. The 50% inhibitory concentration (IC₅₀) of the test compounds against phosphorylation of [CH₃-³H]dThd as the natural substrate for VZV TK, HSV-1 TK and cytosolic TK-1 was determined as described by Balzarini et al.²⁹ Briefly, the activity of purified recombinant nucleoside kinases enzyme were assayed

in a 50 μ L reaction mixture containing 50 mM Tris-HCl, pH 8.0, 2.5 mM MgCl₂, 10 mM dithiothreitol, 2.5 mM ATP, 1.0 mg/mL bovine serum albumin, 10 mM NaF, [CH₃-³H]dThd (0.1 μ Ci in 5 μ L; 1 μ M final concentration), and 5 μ L of recombinant enzyme (containing 7.75 ng of VZV TK or 226 ng of HSV-1 TK or 455 ng of TK-1 protein). The samples were incubated at 37 °C for 30 min in the presence or absence of different concentrations of the test compounds. During this time period, the enzyme reaction proceeded linearly. Aliquots of 45 μ L of the reaction mixtures were spotted on Whatman DE-81 filter paper disks (Whatman, Maidstone, UK). The filters were washed three times for 5 min in 1 mM ammonium formate and once for 5 min in ethanol. The radioactivity on the filters was determined by scintillation counting.

Cytostatic Assay. OST TK⁻/HSV-1-TK⁺, OST TK⁻/VZV TK⁺, and thymidine kinase-negative (OST TK⁻) cells (control cells) were incubated with different concentrations of the compounds in 48-well plates. After culturing for 5 days, the cells were trypsinized and the cell number was determined using a Coulter counter. The CC₅₀ was defined as the compound concentration in μ M required for reducing the cell number by 50%.

Cell-Uptake Studies. A lentiviral vector (LV) encoding the cDNA of VZV-tk linked to the puromycin-*N*-acetyl-transferase (*pac*) gene from *Streptomyces alboniger* through an encephalomyocarditis virus internal ribosome entry sequence (IRES) was produced as described²⁷ and denominated LV-VZVTK-I-P. A similar vector encoding the *E. coli* β -galactosidase (LacZ) gene was used as control (LV-LacZ-I-P).

Human embryonic kidney cells (293T) transduced with LV-VZVTK-I-P and with LV-LacZ-I-P were maintained in cell culture in medium containing 1 μ g/mL puromycin. They were plated in triplicate at a density of 200 000 cells per well in 24-well plates. After 24 h, the medium was discarded and 0.25 mL of fresh medium with HPLC-purified tracer (5 μ Ci of [¹⁸F]-**2** or 30 μ Ci of [¹¹C]-**3** per well) was added. The cells were then incubated at 37 °C in a 5% CO₂ atmosphere for 3 h for [¹⁸F]-**2** and 1 h for [¹¹C]-**3**. Following incubation and removal of medium, the cells were washed three times with 0.4 mL of ice-cold phosphate-buffered saline (PBS). The cells were then lysed with 0.25 mL of Cell Culture Lysis Reagent 1x solution (Promega Corporation, Madison, WI) for 10 min after which the lysate was collected, followed by a 0.125-mL rinse using the same solution. The cell fractions (lysate and rinse) as well as the wash fractions (medium and PBS) were collected separately for each well, and the radioactivity was measured using a gamma counter. The protein concentration of each cell fraction was determined using the Bio-Rad Protein Assay (Biorad, München, Germany) and a spectrophotometer (Bio Synchro-Anthos 2010, Anthos LabTec Instruments, Austria) at 595 nm. The tracer uptake was normalized for total protein content in the cell fraction for each individual well and expressed as percentage of total radioactivity per mg protein.

HPLC Analysis of [¹¹C]-3** Metabolites from VZV-TK-Gene- and LacZ-Gene-Transduced Cells.** VZV-tk and LacZ (control) expressing cells were grown to near confluency in 75-cm² flasks, in the manner and conditions described above. The medium was discarded and the monolayer was incubated with 4.75 mL of fresh medium containing 0.24 mCi of [¹¹C]-**3** for each flask. After 30 min incubation at 37 °C and removal of the supernatant, the cells were washed with cold PBS (3 \times 4 mL). Intracellular components from the cells in both flasks were harvested by treatment with 4 mL of Cell Culture Lysis Reagent solution, followed by a rinse with 1 mL of the same solution. The cell suspension was then centrifuged at 3000 rpm (1837g) for 5 min (Eppendorf centrifuge 5810, Eppendorf). An aliquot of 2 mL of the supernatant was taken and mixed with 25 μ L of a solution of reference compound **3** (0.5 mg/1.5 mL), and the mixture was passed through a preconditioned Oasis cartridge. After connection of the Oasis column to HPLC, it was rinsed by pumping 6 mL of water and the eluate was collected as two 3-mL fractions (fraction no. 2 and 3). The outlet of the Oasis column was then connected to XTerra RP C₁₈ column (5 μ m, 4.6 mm \times 250 mm; Waters); the two columns were eluted using 0.05 M ammonium acetate/acetonitrile (70:30) as the mobile phase at a

flow rate of 1 mL/min. The HPLC eluate was collected as 1-mL fractions, and the radioactivity was measured for all the fractions using a gamma counter (**3**, *t_R* = 8.5 min, fraction no. 11). The supernatant from both flasks was also analyzed in the same manner.

Acknowledgment. The technical assistance of Mrs. Lizette van Berckelaer and Mrs. Ria Van Berwaer is gratefully acknowledged. We thank Prof C. McGuigan, Welsh School of Pharmacy, Cardiff University, for providing the reference compound **4**, and Marva Bex for the synthesis of [¹⁸F]FETBr. We also thank Christelle Terwinghe and Peter Vermaelen for their help during animal experiments. This work was supported by SBO grant (IWT-30 238) of the Flemish Institute supporting Scientific-Technological Research in industry (IWT) and the IDO grant (IDO/02/012) of the Katholieke Universiteit Leuven.

Supporting Information Available: HPLC analysis, melting points, *R_f* values, ¹H NMR and HRMS data for the synthesized compounds. This information is available free of charge via the Internet at <http://pubs.acs.org>.

References

- Penuelas, I.; Boan, J. F.; Marti-Climent, J. M.; Sangro, B.; Mazzolini, G.; Prieto, J.; Richter, J. A. Positron emission tomography and gene therapy: Basic concepts and experimental approaches for in vivo gene expression imaging. *Mol. Imaging Biol.* **2004**, *6*, 225–238.
- Tjuvajev, J. G.; Stockhammer, G.; Desai, R.; Uehara, H.; Watanabe, K.; Gansbacher, B.; Blasberg, R. G. Imaging the expression of transfected genes in vivo. *Cancer Res.* **1995**, *55*, 6126–6132.
- Gambhir, S. S. Molecular imaging of cancer with positron emission tomography. *Nat. Rev. Cancer* **2002**, *2*, 683–693.
- Tjuvajev, J. G.; Doubrovin, M.; Akhurst, T.; Cai, S. D.; Balatoni, J.; Alauddin, M. M.; Finn, R.; Bornmann, W.; Thaler, H.; Conti, P. S.; Blasberg, R. G. Comparison of radiolabeled nucleoside probes (FIAU, FHBG, and FHPG) for PET Imaging of HSV1-tk gene expression. *J. Nucl. Med.* **2002**, *43*, 1072–1083.
- Tjuvajev, J. G.; Macapinlac, H. A.; Daghighian, F.; Scott, A. M.; Ginos, J. Z.; Finn, R. D.; Kothari, P.; Desai, R.; Zhang, J. J.; Beattie, B.; Graham, M.; Larson, S. M.; Blasberg, R. G. Imaging of brain-tumor proliferative activity with iodine-131-iododeoxyuridine. *J. Nucl. Med.* **1994**, *35*, 1407–1417.
- Ryser, J. E.; Blauenstein, P.; Remy, N.; Weinreich, R.; Hasler, P. H.; Novak-Hofer, I.; Schubiger, P. A. [Br-76]Bromodeoxyuridine, a potential tracer for the measurement of cell proliferation by positron emission tomography, in vitro and in vivo studies in mice. *Nucl. Med. Biol.* **1999**, *26*, 673–679.
- Alauddin, M. M.; Conti, P. S.; Mazza, S. M.; Hamzeh, F. M.; Lever, J. R. Synthesis of 9-[3-[F-18]-fluoro-1-hydroxy-2-propoxy)methyl]-guanine ([F-18]-FHPG): A potential imaging agent of viral infection and gene therapy using PET. *Nucl. Med. Biol.* **1996**, *23*, 787–792.
- Alauddin, M. M.; Conti, P. S. Synthesis and preliminary evaluation of 9-[4-[F-18]-fluoro-3-hydroxymethylbutyl]guanine ([F-18]FHBG): A new potential imaging agent for viral infection and gene therapy using PET. *Nucl. Med. Biol.* **1998**, *25*, 175–180.
- Alauddin, M. M.; Shahinian, A.; Park, R.; Tohme, M.; Fissekis, J. D.; Conti, P. S. Synthesis and evaluation of 2'-deoxy-2'-F-18-fluoro-5-fluoro-1-beta-D-arabinofuranosyluracil as a potential PET imaging agent for suicide gene expression. *J. Nucl. Med.* **2004**, *45*, 2063–2069.
- Yaghoubi, S.; Barrio, J. R.; Dahlbom, M.; Iyer, M.; Namavari, M.; Goldman, R.; Herschman, H. R.; Phelps, M. E.; Gambhir, S. S. Human pharmacokinetic and dosimetry studies of [F-18]FHBG: A reporter probe for imaging herpes simplex virus type-1 thymidine kinase reporter gene expression. *J. Nucl. Med.* **2001**, *42*, 1225–1234.
- Yaghoubi, S. S.; Couto, M. A.; Chen, C. C.; Polavaram, L.; Cui, G. G.; Sen, L. Y.; Gambhir, S. S. Preclinical safety evaluation of F-18-FHBG: A PET reporter probe for imaging herpes simplex virus type 1 thymidine kinase (HSV1-tk) or mutant HSV1-sr39tk's expression. *J. Nucl. Med.* **2006**, *47*, 706–715.
- Serganova, I.; Blasberg, R. Reporter gene imaging: potential impact on therapy. *Nucl. Med. Biol.* **2005**, *32*, 763–780.
- Herschman, H. R. PET reporter genes for noninvasive imaging of gene therapy, cell tracking and transgenic analysis. *Crit. Rev. Oncol. Hematol.* **2004**, *51*, 191–204.

- (14) Dishino, D. D.; Welch, M. J.; Kilbourn, M. R.; Raichle, M. E. Relationship between lipophilicity and brain extraction of C-11-labeled radiopharmaceuticals. *J. Nucl. Med.* **1983**, *24*, 1030–1038.
- (15) Young, R. C.; Mitchell, R. C.; Brown, T. H.; Ganellin, C. R.; Griffiths, R.; Jones, M.; Rana, K. K.; Saunders, D.; Smith, I. R.; Sore, N. E.; Wilks, T. J. Development of a new physicochemical model for brain penetration and its application to the design of centrally acting H-2-receptor histamine-antagonists. *J. Med. Chem.* **1988**, *31*, 656–671.
- (16) Shiue, G. G.; Shiue, C. Y.; Lee, R. L.; MacDonald, D.; Hustinx, R.; Eck, S. L.; Alavi, A. A. A simplified one-pot synthesis of 9-[(3-[F-18]fluoro-1-hydroxy-2-propoxy)methyl]guanine ([F-18]FHPG) and 9-(4-[F-18]fluoro-3-hydroxymethylbutyl)guanine ([F-18]FHBG) for gene therapy. *Nucl. Med. Biol.* **2001**, *28*, 875–883.
- (17) McGuigan, C.; Yarnold, C. J.; Jones, G.; Velazquez, S.; Barucki, H.; Brancale, A.; Andrei, G.; Snoeck, R.; De Clercq, E.; Balzarini, J. Potent and selective inhibition of varicella-zoster virus (VZV) by nucleoside analogues with an unusual bicyclic base. *J. Med. Chem.* **1999**, *42*, 4479–4484.
- (18) McGuigan, C.; Brancale, A.; Barucki, H.; Srinivasan, S.; Jones, G.; Pathirana, R.; Carangio, A.; Blewett, S.; Luoni, G.; Bidet, O.; Jukes, A.; Jarvis, C.; Andrei, G.; Snoeck, R.; De Clercq, E.; Balzarini, J. Furano pyrimidines as novel potent and selective anti-VZV agents. *Antiviral Chem. Chemother.* **2001**, *12*, 77–89.
- (19) Sienaert, R.; Naesens, L.; Brancale, A.; De Clercq, E.; McGuigan, C.; Balzarini, J. Specific recognition of the bicyclic pyrimidine nucleoside analogs, a new class of highly potent and selective inhibitors of varicella-zoster virus (VZV), by the VZV-encoded thymidine kinase. *Mol. Pharmacol.* **2002**, *61*, 249–254.
- (20) Balzarini, J.; McGuigan, C. Chemotherapy of varicella-zoster virus by a novel class of highly specific anti-VZV bicyclic pyrimidine nucleosides. *Biochim. Biophys. Acta* **2002**, *1587*, 287–295.
- (21) McGuigan, C.; Barucki, H.; Blewett, S.; Carangio, A.; Erichsen, J. T.; Andrei, G.; Snoeck, R.; De Clercq, E.; Balzarini, J. Highly potent and selective inhibition of varicella-zoster virus by bicyclic furopyrimidine nucleosides bearing an aryl side chain. *J. Med. Chem.* **2000**, *43*, 4993–4997.
- (22) Zhang, M. R.; Tsuchiyama, A.; Haradahira, T.; Yoshida, Y.; Furutsuka, K.; Suzuki, K. Development of an automated system for synthesizing ¹⁸F-labeled compounds using [¹⁸F]fluoroethyl bromide as a synthetic precursor. *Appl. Radiat. Isot.* **2002**, *57*, 335–342.
- (23) Larsen, P.; Ulin, J.; Dahlstrom, K.; Jensen, M. Synthesis of [¹¹C]-iodomethane by iodination of [¹¹C]methane. *Appl. Radiat. Isot.* **1997**, *48*, 153–157.
- (24) Mallet, C. R.; Mazzeo, J. R.; Neue, U. Evaluation of several solid phase extraction liquid chromatography/tandem mass spectrometry on-line configurations for high-throughput analysis of acidic and basic drugs in rat plasma. *Rapid Commun. Mass Spectrom.* **2001**, *15*, 1075–1083.
- (25) Balzarini, J.; Sienaert, R.; Liekens, S.; Van Kuilenburg, A.; Carangio, A.; Esnouf, R.; De Clercq, E.; McGuigan, C. Lack of susceptibility of bicyclic nucleoside analogs, highly potent inhibitors of varicella-zoster virus, to the catabolic action of thymidine phosphorylase and dihydropyrimidine dehydrogenase. *Mol. Pharmacol.* **2002**, *61*, 1140–1145.
- (26) Balzarini, J.; McGuigan, C. Bicyclic pyrimidine nucleoside analogues (BCNAs) as highly selective and potent inhibitors of varicella-zoster virus replication. *J. Antimicrob. Chemother.* **2002**, *50*, 5–9.
- (27) Geraerts, M.; Michiels, M.; Baekelandt, V.; Debyser, Z.; Gijsbers, R. Upscaling of lentiviral vector production by tangential flow filtration. *J. Gene Med.* **2005**, *7*, 1299–1310.
- (28) Fritzberg, A. R.; Whitney, W. P.; Kuni, C. C.; Klingensmith, W. Biodistribution and renal excretion of ^{99m}Tc-N, N'-bis-(Mercaptoacetamido) ethylenediamine. Effect of renal tubular transport inhibitors. *Int. J. Nucl. Med. Biol.* **1982**, *9*, 79–82.
- (29) Balzarini, J.; Celen, S.; Karlsson, A.; de Groot, T.; Verbruggen, A.; Bormans, G. The effect of a methyl or 2-fluoroethyl substituent at the N-3 position of thymidine, 3'-fluoro-3'-deoxythymidine and 1-beta-D-arabinosylthymine on their antiviral and cytostatic activity in cell culture. *Antiviral Chem. Chemother.* **2006**, *17*, 17–23.

JM060964M